Author for correspondence:
Hany W. Darwish
e-mail: hdarwish@ksu.edu.sa

Identification of reactive intermediate formation and bioactivation pathways in Abemaciclib metabolism by LC–MS/MS: *in vitro* metabolic investigation

Adnan A. Kadi[1], Hany W. Darwish[1,2], Hatem A. Abuelizz[1], Thamer A. Alsubi[1] and Mohamed W. Attwa[1]

[1]Department of Pharmaceutical Chemistry, College of Pharmacy, King Saud University, PO Box 2457, Riyadh 11451, Saudi Arabia
[2]Analytical Chemistry Department, Faculty of Pharmacy, Cairo University, Kasr El-Aini Street, Cairo 11562, Egypt

HWD, 0000-0002-3437-2748; MWA, 0000-0002-1147-4960

Abemaciclib (Verzenio®) is approved as a tyrosine kinase inhibitor (TKI) for breast cancer treatment. In this study, *in vitro* phase I metabolic profiling of Abemaciclib (ABC) was done using rat liver microsomes (RLMs). We checked the formation of reactive intermediates in ABC metabolism using RLMs in the presence of potassium cyanide (KCN) that was used as a capturing agent for iminium reactive intermediates forming a stable complex that can be characterized by LC–MS/MS. Nine *in vitro* phase I metabolites and three cyano adducts were identified. The metabolic reactions involved in the formation of these metabolites and adducts are reduction, oxidation, hydroxylation and cyanide addition. The bioactivation pathway was also proposed. Knowing the electrodeficient bioactive centre in ABC structure helped in making targeted modifications to improve its safety and retain its efficacy. Blocking or isosteric replacement of α-carbon to the tertiary nitrogen atoms of piperazine ring can aid in reducing toxic side effects of ABC. No previous articles were found about *in vitro* metabolic profiling for ABC or structural identification of the formed reactive metabolites for ABC.

1. Introduction

A malignant tumour is formed of a group of cancer cells that have the ability to grow and invade tissues either surrounding or at

Abemaciclib

molecular weight: 506.61
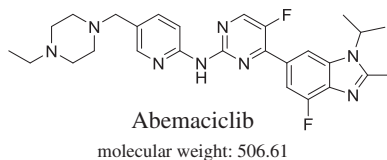
Figure 1. ABC chemical structure.

**Table 1.** List of chemicals and materials.

name	source
Abemaciclib	Med. Chem. Express (NJ, USA)
acetonitrile (HPLC grade), ammonium formate, potassium cyanide and formic acid	Sigma-Aldrich (USA)
water (HPLC grade)	Milli-Q plus filtration system (USA)
rats (Sprague-Dawley)	King Saud University experimental animal care center (Saudi Arabia)

distant areas of the body [1]. Globally, breast cancer is the most frequently diagnosed cancer in women; it affects about 12% of women worldwide [2]. Saudi Arabia is no exception, where breast cancer is most commonly prevalent. It accounts for about 22% of all new cancers in women that are ranked first figures [3]. There is a group of novel drugs that specifically target gene changes in cancer cells that help the cells grow or spread. Tyrosine kinases (TKs) are important targets because of their important role in the modulation of growth factor signalling [4]. Controlling the activity of TK in the cell regulates many vital processes such as cell cycle, proliferation and cell death [5].

Cyclin-dependent kinases 4 and 6 (CDK4/6), as a class of tyrosine kinase inhibitor (TKI), play a crucial role in cell proliferation. When CDK4/6 pathway is dysregulated, it leads to an implication in breast cancer biology [6]. There are three highly selective CDK4/6 inhibitors that have been approved for breast cancer therapy: Palbociclib, Ribociclib and Abemaciclib (ABC) (Verzenio®) [7]. ABC (figure 1) is the third agent in this class, which was approved in September 2017 by the Food and Drug Administration (FDA), either in combination with fulvestrant for women or as monotherapy for women and men with HR-positive, HER2-negative advanced or metastatic breast cancer. Lately, in February 2018, FDA approved ABC with an aromatase inhibitor as the first-line endocrine-based therapy for metastatic breast cancer. The most frequent side effects of the drug were diarrhoea, which occurred in approximately 80% of patients, neutropenia, fatigue, infections, nausea, abdominal pain, anaemia, vomiting, alopecia, decreased appetite and leukopenia [8].

Our group previously studied reactive metabolite formations of some TKI drugs. The current work proved that ABC formed three reactive intermediates through a specific bioactivation pathway. KCN was used as a trapping agent to capture the formed reactive metabolites and the bioactivation pathways were characterized [8–12]. The chemical structures of ABC contain N-ethyl piperazine ring. This group is expected to undergo metabolism generating reactive iminium intermediates that can be trapped by KCN forming cyano adducts. Oxidation at a carbon alpha to an N-substituted piperazine ring is known to result in iminium ions, which are considered hard electrophiles and can be trapped by cyanide anions to form cyano adducts. The N-substituted piperazine partial structures become bioactivated and subsequently trapped by the nucleophilic cyanide anion. The reactive intermediates were postulated as imine and imine-carbonyl conjugate (α,β-unsaturated) structures on the piperazine ring. Bioactivation of the N-substituted piperazine partial structure, which can be characterized and detected using tandem mass spectrometry (LC–MS/MS), is a possible explanation for reported idiosyncratic toxicity [13–16].

Iminium intermediates initiate several toxic side effects through previously reported mechanisms as in the case of brigatinib and ponatinib that bind covalently to a DNA base [9,17]. Knowing the electrodeficient bioactive centre in ABC structure helped in making targeted modifications to improve its safety and retain its efficacy. ABC rat liver microsome (RLM) incubation resulted in the identification of nine *in vitro* phase I metabolites and three cyano conjugates, and the proposed reactions involved include reduction, oxidation, hydroxylation and cyanide addition.

(a)

(b)
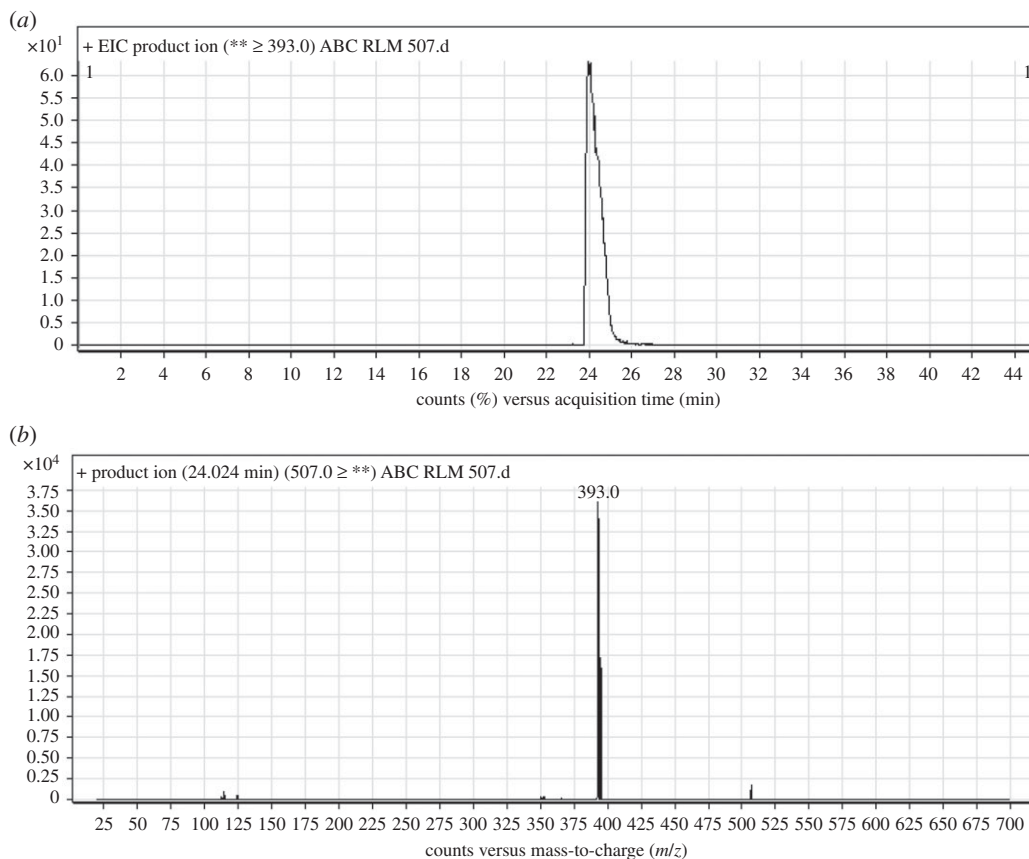
**Figure 2.** ABC PI chromatogram (a) and ABC PI MS spectrum (b).

Table 2. Chromatographic parameters of the proposed LC–MS/MS methodology.

liquid chromatography			mass spectrometry	
RRLC	Agilent 1200 series		mass spectrometer	Agilent 6410 QQQ
mobile phase	A: 0.1% formic acid		ESI source	positive ESI
	B: ACN			N_2 of low purity as drying gas: At flow
	flow rate: 0.25 ml min^{-1}			rate of 12 l min^{-1} and 60 psi pressure
	run time: 75 min			
Agilent Zorbax eclipse	L	150 mm		ESI temperature: 350°C
plus C_{18} column	ID	2.1 mm		capillary voltage: 4000 V
	PS	3.5 μm	gas inside collision cell	N_2 of high purity
	T	22 ± 1°C	detection modes	MS scan and PI
elution system	time in minutes	% ACN	drug	ABC and its in vitro and reactive metabolites
	0	5		
	5	5	fragmentation	fragmentor voltage (FV): 135 V
	30	60		collision energy (CE): 20 eV
	40	90		
	45	5		

2. Chemicals and methods

2.1. Chemicals

All chemicals are described in table 1. RLMs were made in house using Sprague-Dawley rats following previously reported methods [9,17–19]. The experimental design for animal work was approved by the University's Ethics Review Committee.
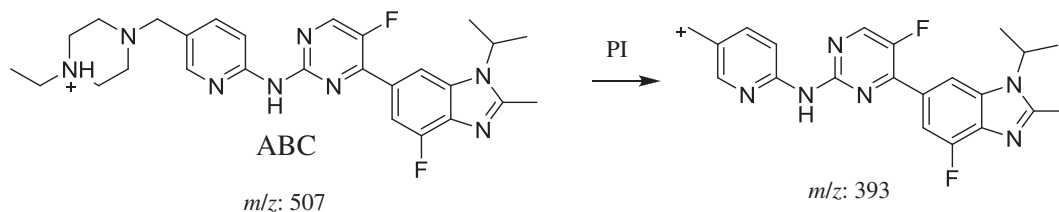
Scheme 1. PIs of ABC.

Table 3. Identified *in vitro* and cyano adducts of ABC.

|	MS scan	MS^2 product ions	t_R (min)	proposed phase 1 metabolic reaction
ABC	507	393	23.9	
In vitro ABC metabolism				
ABC493a	493	378.8	22.8	demethylation
ABC493b	493	378.9	25.8	demethylation
ABC509	509	395.1, 509	24.3	reduction
ABC521	521	365, 406.5, 521	28.8	methyl oxidation
ABC523a	523	393	23.2	ethyl hydroxylation
ABC523b	523	130, 393, 421, 495, 523	26.5	piperazine hydroxylation
ABC525a	525	395.1	23.32	hydroxylation and reduction
ABC525b	525	395.1	26.4	hydroxylation and reduction
ABC537	537	392.5	30.74	hydroxylation and oxidation
cyano adducts				
ABC532a	532	392.9	26.5	cyanide addition
ABC532b	532	393	37.2	cyanide addition
ABC548	548	393	29.36	hydroxylation and cyanide addition

2.2. Chromatographic conditions

An Agilent 6410 QQQ equipped with an ESI coupled to an Agilent 1200 HPLC was used. The liquid and mass chromatographic parameters were adjusted for each drug. ABC and its metabolites were produced in the collision cell by CID. The optimized conditions for chromatographic resolution of incubation mixture extract are given in table 2.

2.3. RLM incubations

ABC was incubated at 20 µM with 1 mg ml^{-1} RLMs, 1 mM NADPH, 1 mM KCN and 50 mM Na/K phosphate buffer (pH 7.4) containing 3.3 mM MgCl$_2$. The mixtures were incubated at 37°C in a shaking water bath for 60 min before the metabolic reactions were terminated using protein precipitation by adding 2 ml of ice-cold ACN followed by centrifugation at 9000 g for 10 min at 4°C. The supernatants were removed to clean vials then evaporated to dryness, reconstituted in the mobile phase and analysed by the LC/MS system [8,12,17,20]. Two controls were done in the absence of NADPH or RLMs to confirm that ABC phase I metabolites were metabolically formed.

2.4. Characterization of ABC reactive intermediates in *in vitro* metabolic reactions
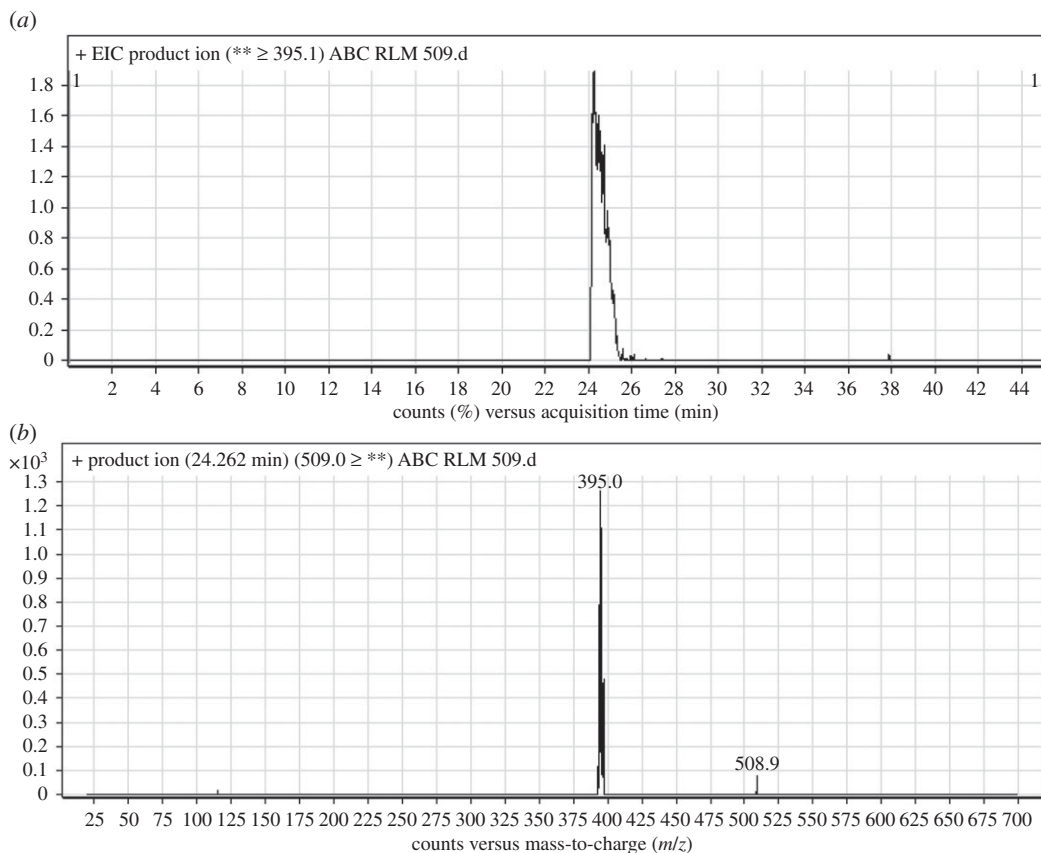
The same RLM metabolic incubation with ABC, previously described in §2.3, was repeated but in addition to 1.0 mM KCN to trap reactive iminium intermediates. This experiment was repeated three
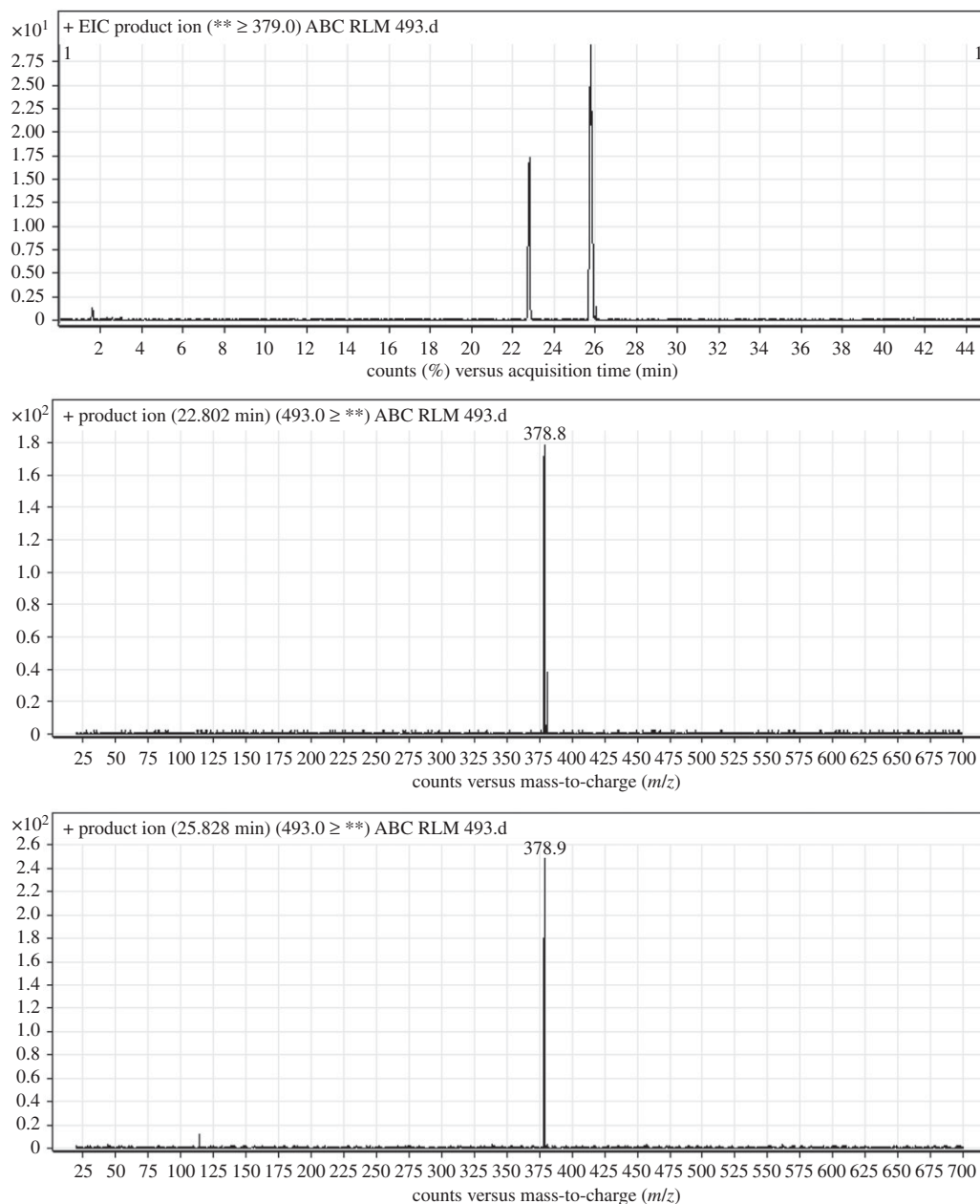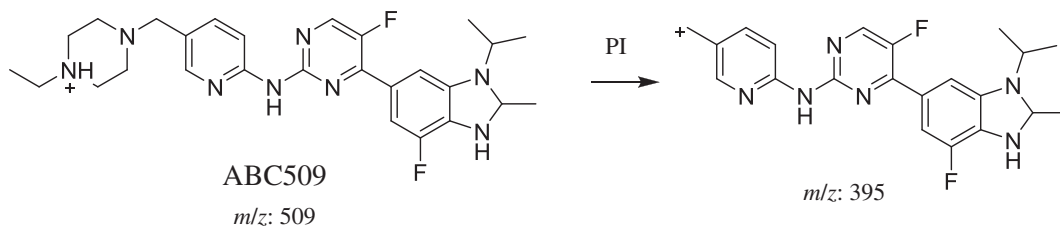
Figure 3. ABC493 PI chromatogram (*a*), ABC493a PI MS spectrum (*b*) and ABC493b PI MS spectrum (*c*).
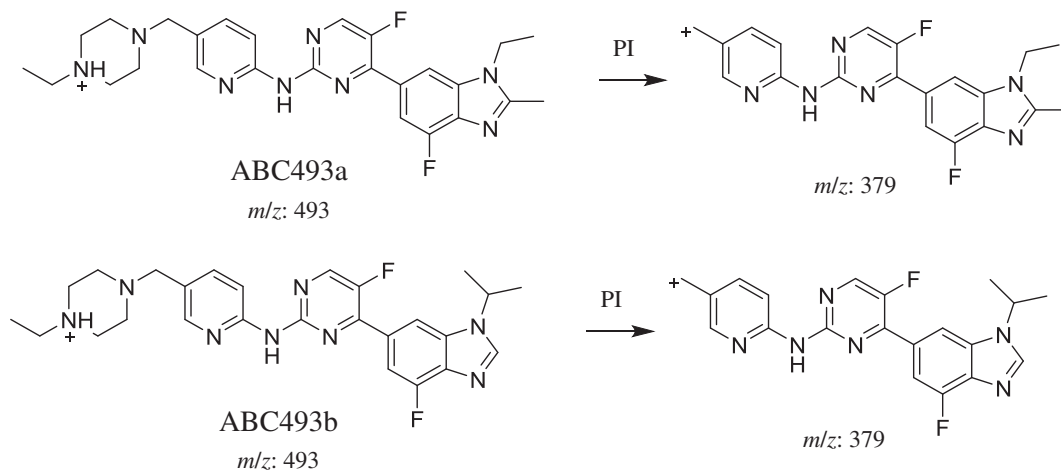
Scheme 2. PIs of ABC493a and ABC493b.

(a)

(b)

Figure 4. ABC509 PI chromatogram (a) and ABC509 PI MS spectrum (b).

Scheme 3. PIs of ABC509.

times to confirm the results and support our conclusions. Two controls were done in the absence of NADPH or KCN to confirm that cyano adducts are formed due to metabolic bioactivation.
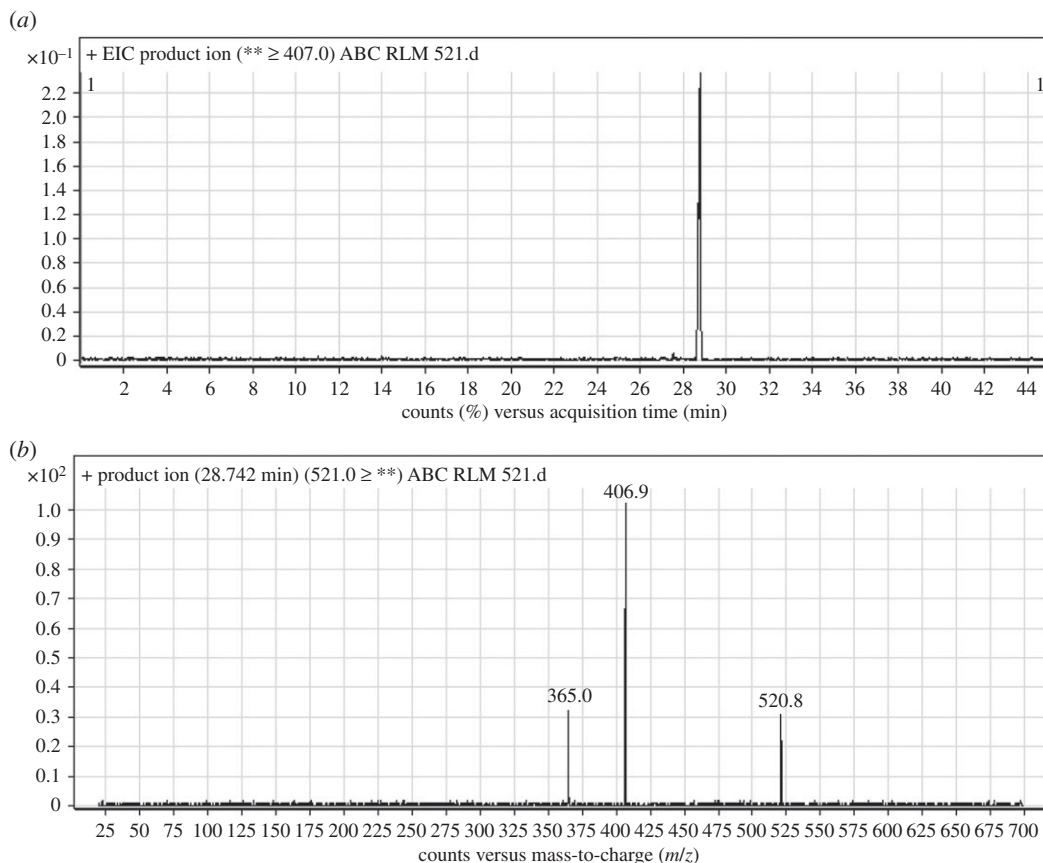
2.5. Identification of ABC reactive metabolites

MS scan and extracted ion chromatogram (EIC) detection modes were used to characterize and locate metabolites in the incubation mixtures, while product ion (PI) was used to identify ABC *in vitro* metabolites and adducts of reactive intermediates formed in ABC metabolism. Locating metabolites in metabolic mixture extract chromatogram was performed by EIC of *m/z* of the supposed ABC metabolites.
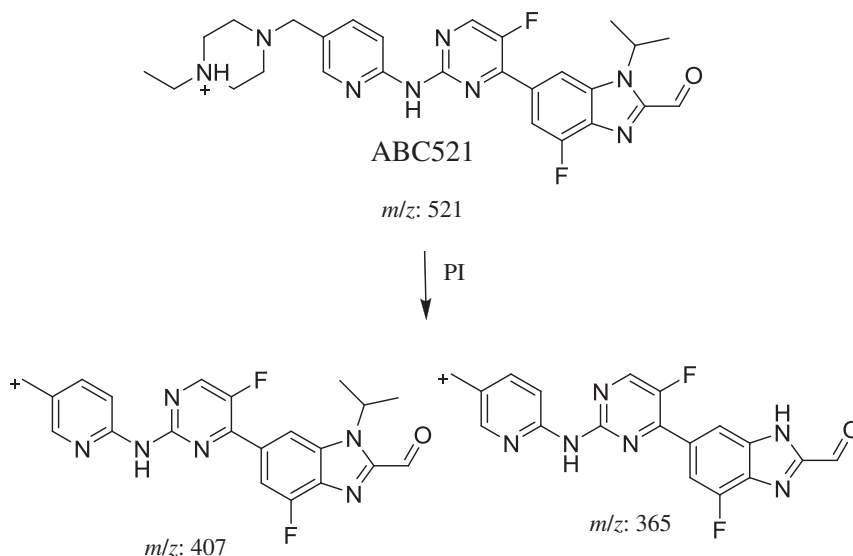
3. Results and discussion

3.1. PI study of ABC

ABC chromatographic peak appears at 24.0 min in PI chromatogram (figure 2a). Collision-induced dissociation (CID) of ABC at *m/z* 507 generates one fragment ion (FI) at *m/z* 399 by the loss of ethyl piperazine moiety (figure 2b and scheme 1).
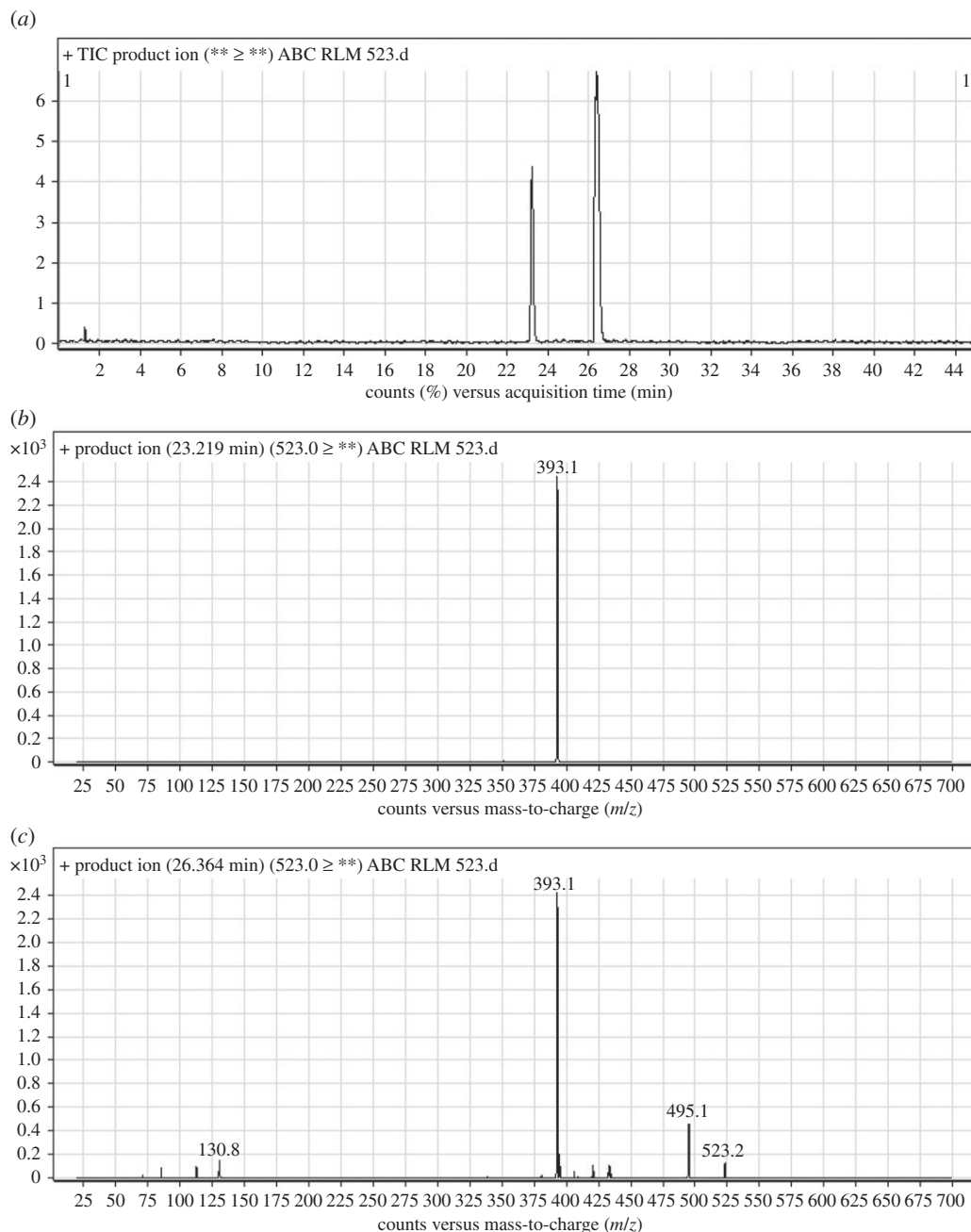
Figure 5. ABC521 PI chromatogram (*a*) and ABC521 PI MS spectrum (*b*).

Scheme 4. PIs of ABC521.

3.2 Identification of *in vitro* and reactive ABC metabolites

After the purification and extraction of ABC RLM incubations, 15 µl was injected into LC−MS/MS. ABC incubation led to the identification of nine *in vitro* phase I metabolites and three cyano adducts, and the proposed reactions involved include reduction, oxidation, hydroxylation and cyanide addition (table 3). All these metabolites were formed in all incubations when repeated three times; this confirmed the

Figure 6. ABC523 PI chromatogram (*a*), ABC523a PI MS spectrum (*b*) and ABC523b PI MS spectrum (*c*).

validity of the used method. These results were confirmed by the absence of identified phase I metabolites and cyano adducts in all controls.

3.2.1. Identification of ABC493a and ABC493b phase I metabolites of ABC

ABC493a and ABC493b chromatographic peaks appear at 22.8 and 25.8 min, respectively, in PI chromatogram (figure 3*a*). CID of AB493 generates one FI at m/z 379 (figure 3*b,c*). Comparing with PIs of ABC, a decrease of 14 m/z units was identified, which indicates that demethylation metabolic reaction occurred in benzimidazole ring (scheme 2).

3.2.2. Identification of ABC509 phase I metabolite of ABC

ABC509 chromatographic peak appears at 24.3 min in PI chromatogram (figure 4*a*). CID of ABC509 generates one FI at m/z 395 (figure 4*b*). Compared with PIs of ABC, an increase of 2 m/z
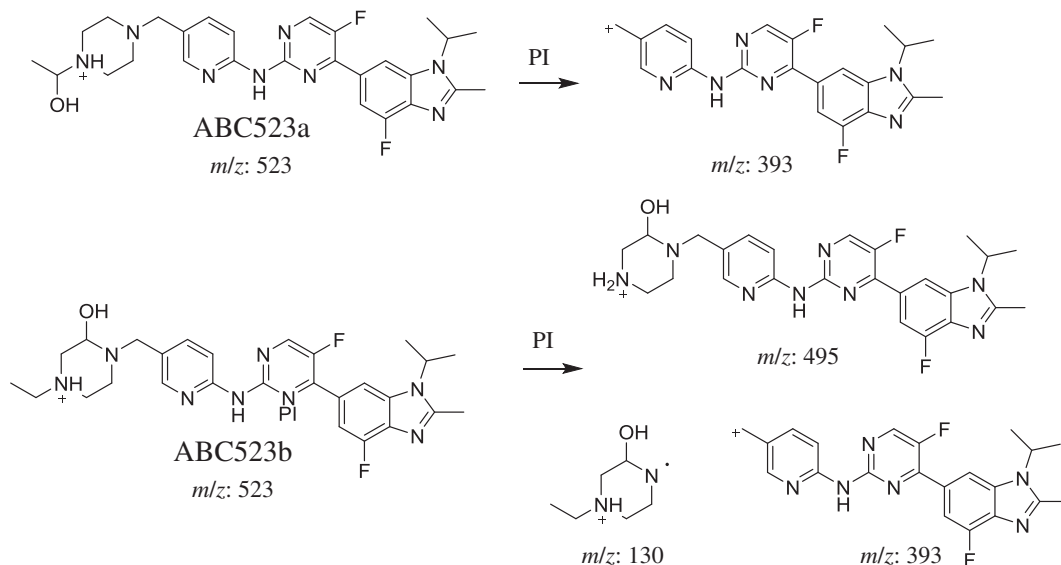
Scheme 5. PIs of ABC523a and ABC523b.

units was identified, which indicates that reduction metabolic reaction occurred in benzimidazole ring (scheme 3).

3.2.3. Identification of ABC521 phase I metabolite of ABC

ABC521 chromatographic peak appears at 28.7 min in PI chromatogram (figure 5a). CID of ABC521 generates two FIs at m/z 407 and m/z 365 (figure 5b). Compared with PIs of ABC, an increase of 14 m/z units was identified, which indicates that oxidation metabolic reaction occurred in benzimidazole ring (scheme 4).

3.2.4. Identification of ABC523a and ABC523b phase I metabolites of ABC

ABC523a and ABC523b chromatographic peaks appeared at 23.2 and 26.4 min, respectively, in PI chromatogram (figure 6a). CID of ABC523a generates one FI at m/z 393 (figure 6b). CID of ABC523b generates three FIs at m/z 495, m/z 393 and m/z 130 (figure 6c). Compared with PIs of ABC, an increase of 16 m/z units was identified, which indicates that hydroxylation metabolic reaction occurred in N-ethyl piperazine ring (scheme 5).

### 3.2.5. Identification of ABC525a and ABC525b phase I metabolites of ABC

ABC525a and ABC525b chromatographic peaks appeared at 23.3 and 26.4 min, respectively, in PI chromatogram (figure 7a). CID of ABC525 metabolites generates one FI at m/z 395 (figure 7b,c). Compared with PIs of ABC, an increase of 18 m/z units was identified, which indicates that reduction metabolic reaction occurred in benzimidazole ring in addition to hydroxylation metabolic reaction that occurred in N-ethyl piperazine ring (scheme 6).

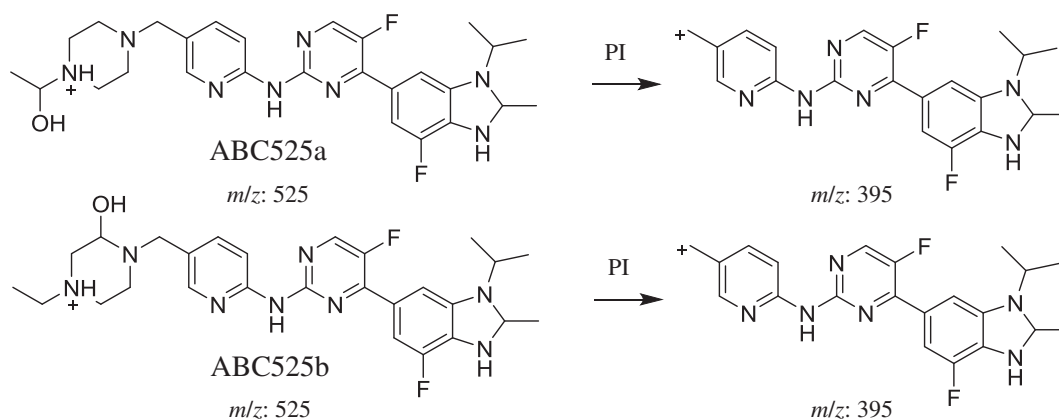### 3.2.6. Identification of ABC537 phase I metabolite of ABC

ABC537 chromatographic peak appears at 30.7 min in PI chromatogram (figure 8a). CID of ABC537 generates one FI at m/z 393 (figure 8b). Compared with PIs of ABC, an increase of 30 m/z units was identified, which indicates hydroxylation and oxidation metabolic reactions occurred in N-ethyl piperazine ring (scheme 7).

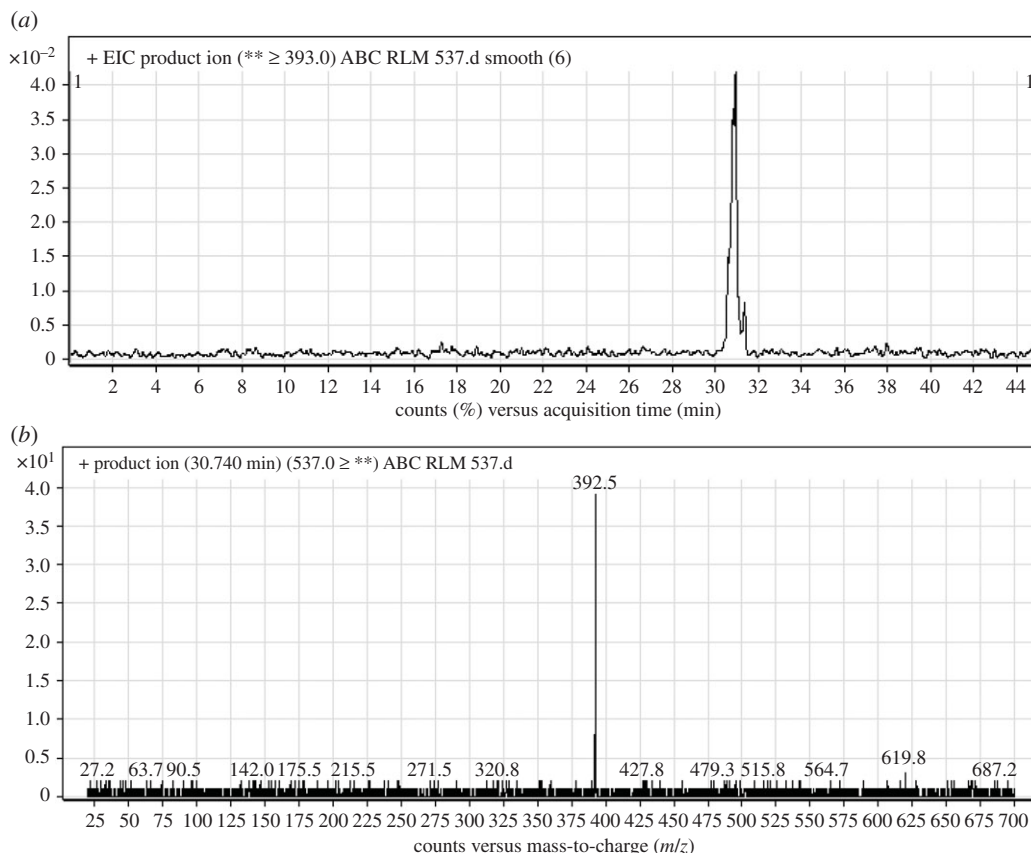### 3.2.7. Identification of ABC532a and ABC532b cyano adducts of ABC

ABC532a and ABC532b chromatographic peaks appeared at 26.8 and 37.2 min, respectively, in PI chromatogram (figure 9a). CID of ABC532 metabolites generates one FI at m/z 393 (figure 9b,c).
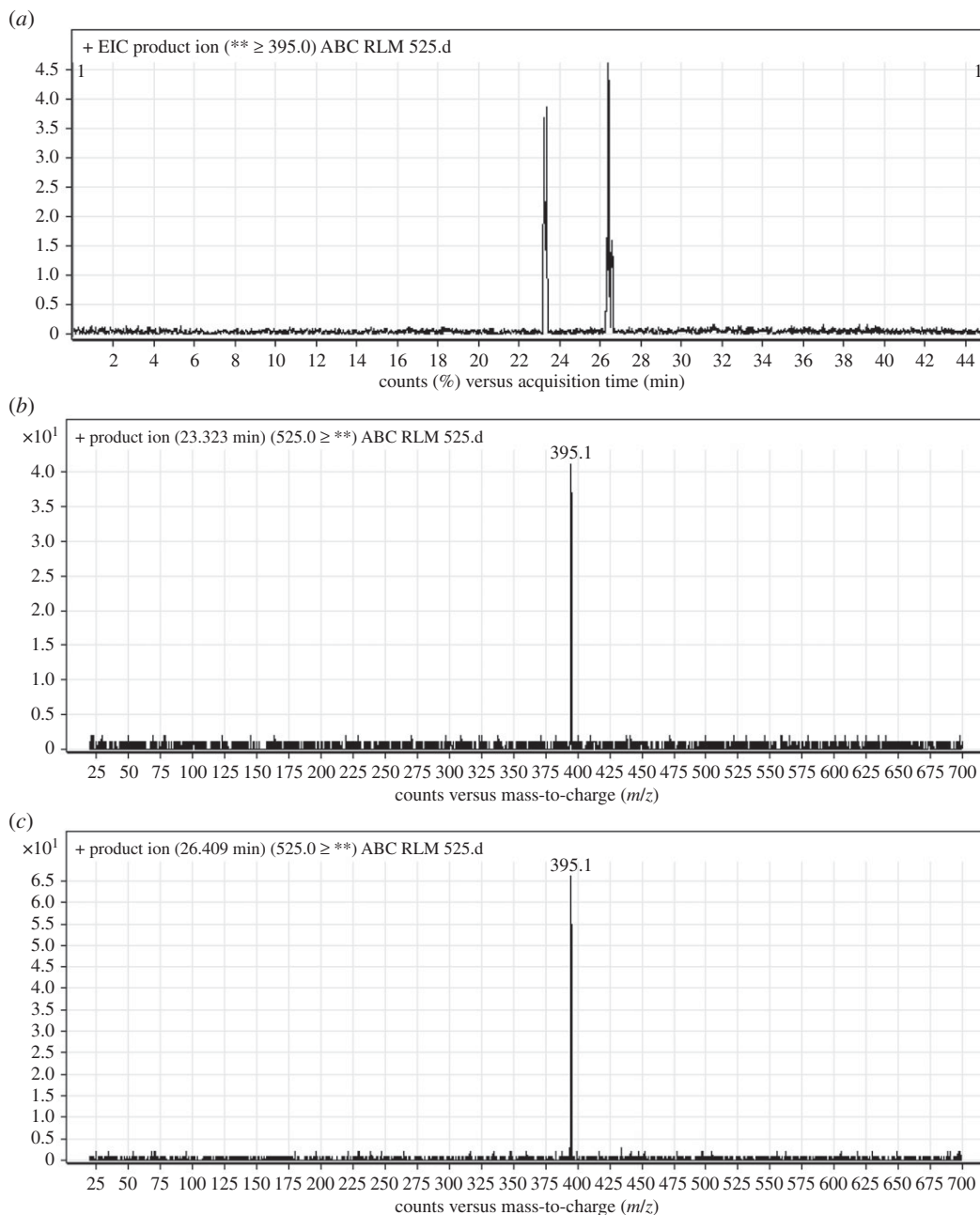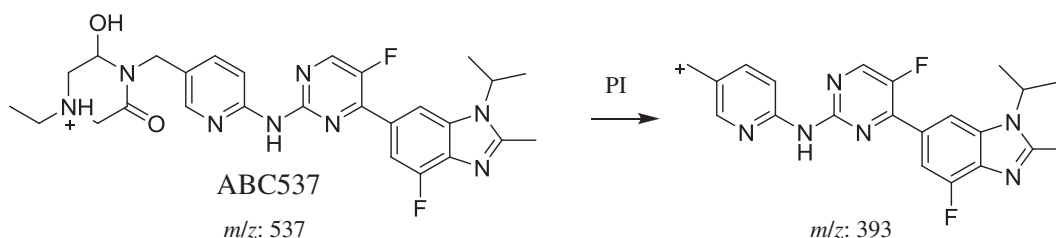
Figure 7. ABC525 PI chromatogram (*a*), ABC525a PI MS spectrum (*b*) and ABC525b PI MS spectrum (*c*).

Scheme 6. PIs of ABC525a and ABC525b.

Figure 8. ABC537 PI chromatogram (*a*) and ABC537 PI MS spectrum (*b*).


Scheme 7. PIs of ABC537.

Compared with PIs of ABC, PI at *m*/*z* 393 indicates that all metabolic changes occurred in *N*-ethyl piperazine ring. An increase of 25 *m*/*z* units indicates that cyano addition occurred in *N*-ethyl piperazine ring (scheme 8).

### 3.2.8. Identification of ABC548 cyano adduct of ABC

ABC548 chromatographic peak appears at 29.4 min in PI chromatogram (figure 10*a*). CID of ABC548 generates one FI at *m*/*z* 393 (figure 10*b*). Compared with PIs of ABC, PI at *m*/*z* 393 indicates that all metabolic changes occurred in *N*-ethyl piperazine ring. An increase of 41 *m*/*z* units indicates that hydroxylation and cyano addition occurred in *N*-ethyl piperazine ring (scheme 9).

3.3. Supposed pathways of bioactivation of ABC

Scheme 10 shows the different pathways for bioactivation of ABC. The formation of ABC532a, ABC532b and ABC548 cyanide adducts confirmed the formation of iminium intermediates in piperazine ring
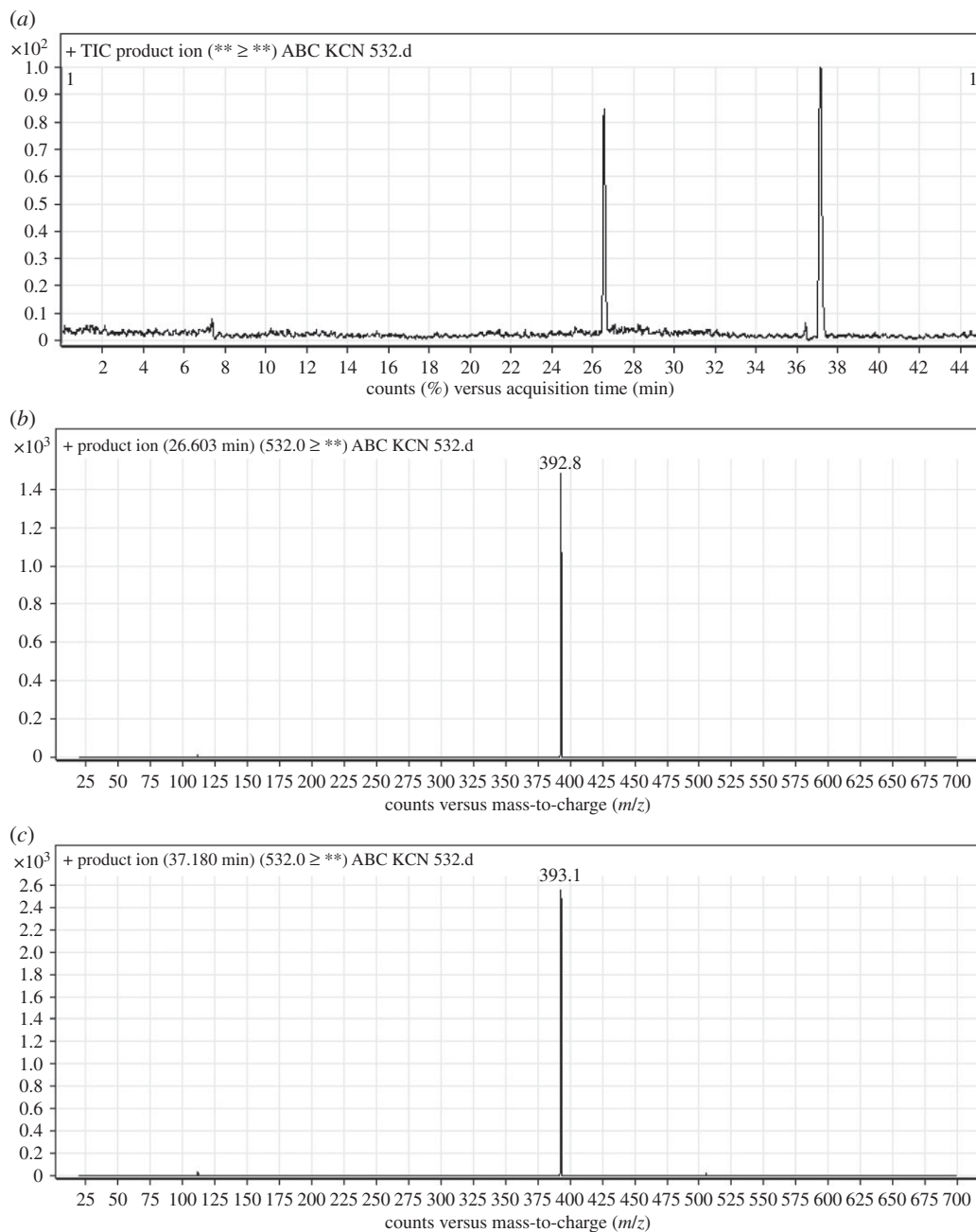
Figure 9. ABC532 PI chromatogram (*a*), ABC532a PI MS spectrum (*b*) and ABC532b PI MS spectrum (*c*).
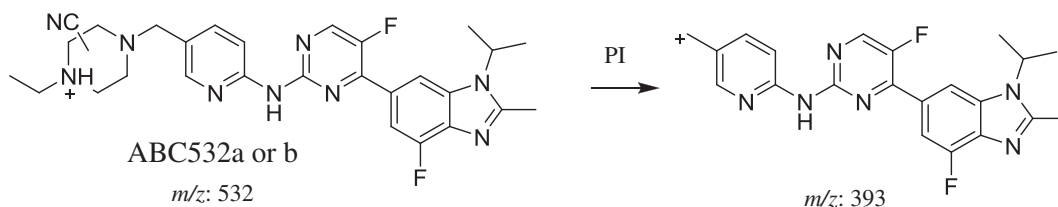

Scheme 8. PIs of ABC532a and ABC532b.

metabolism. Hydroxylation of piperazine ring in ABC followed by dehydration resulted in the generation of iminium ion intermediates that are unstable and reactive that can be trapped by cyanide-forming stable adduct which can be detected in LC–MS/MS. The formation pathway of
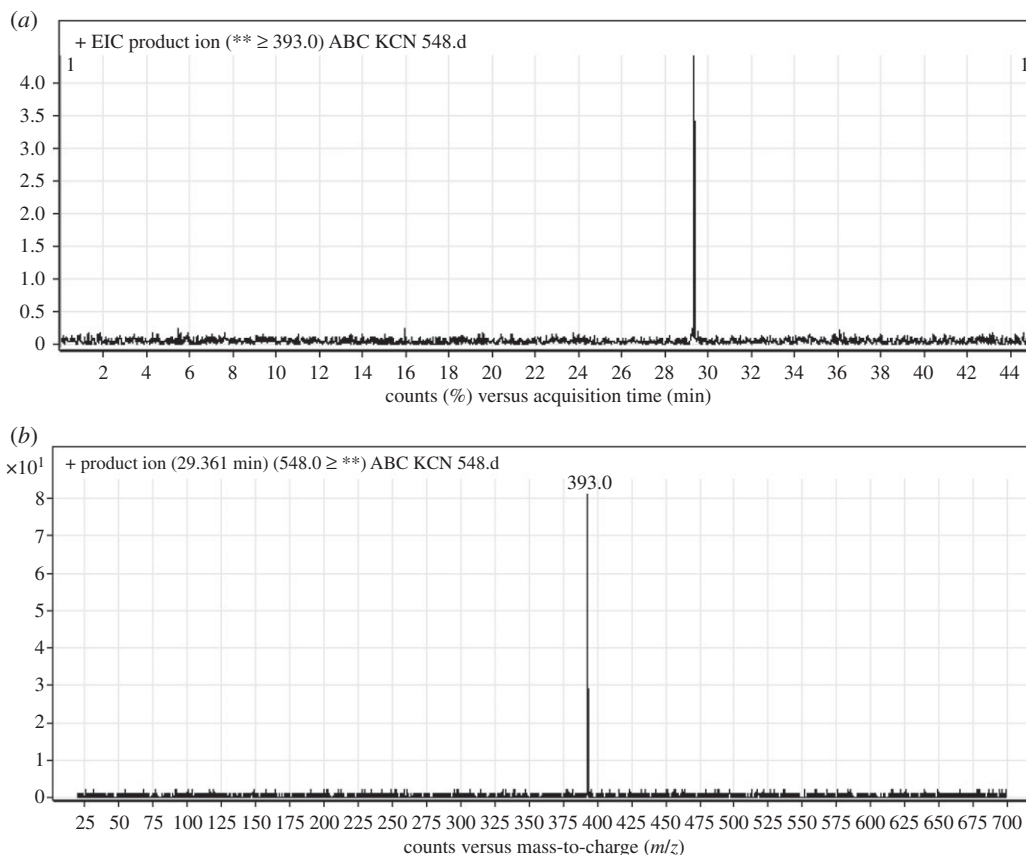
Figure 10. ABC548 PI chromatogram (*a*) and ABC548 PI MS spectrum (*b*).
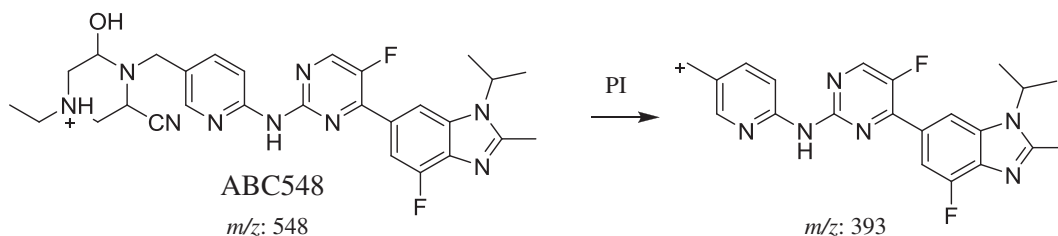

Scheme 9. PIs of ABC548.

iminium intermediate and bioactivation mechanism of ABC was previously described with cyclic tertiary amine-containing drugs [10,11,17,20].

4. Conclusion

Three potential iminium reactive metabolites were detected and the bioactivation pathways were proposed (figure 11). Nine *in vitro* phase I metabolites were identified. The findings of potentially reactive intermediates of these drugs may give a deeper understanding of their adverse effects. Further drug discovery studies in ABC structure can shed more light on the possibility of blocking or reducing the formation of reactive intermediates by introducing alkyl substituents or isosteric replacement to the alpha position of the piperazine partial moiety which would probably block or interrupt enzymatic oxidation/hydroxylation on α-carbon atoms. This study opens the way for new drug development with more safety profile.

Ethics. Male Sprague-Dawley rats were maintained according to the Animal Care Center instructions at KSU that were accepted by the Local Animal Care and Use Committee of KSU. The animal experimental design used in
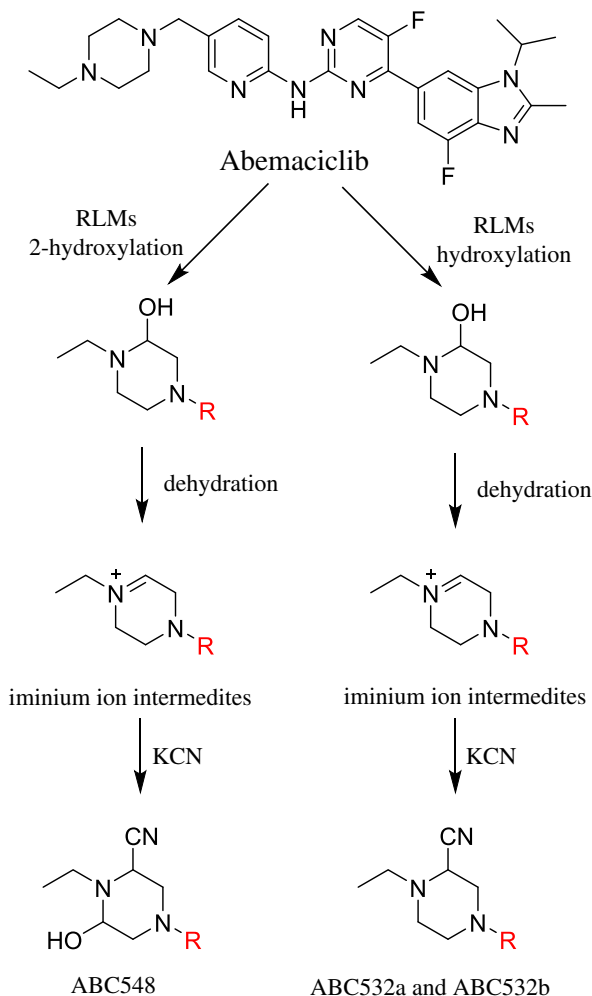
Scheme 10. Proposed pathways for the iminium intermediate generation and trapping strategy.
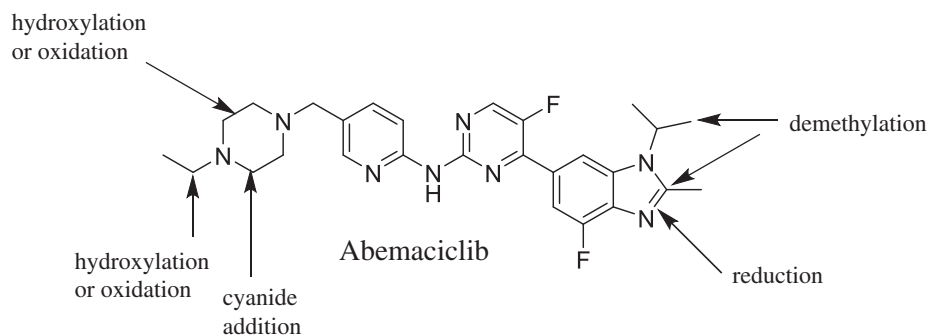
Figure 11. *In vitro* metabolic pathways and bioactivation centres of ABC.

the current work was approved by the University's Ethics Review Committee. Informed consent was taken from all participants.

References

1. American Cancer Society. 2016 See http://www.cancer.org/acs/groups/cid/documents/webcontent/003090-pdf.pdf (accessed 31 October 2018).

2. McGuire A, Brown JA, Malone C, McLaughlin R, Kerin MJ. 2015 Effects of age on the detection and management of breast cancer. *Cancers* **7**, 908–929. (doi:10.3390/cancers7020815)

3. National Campaign for Breast Cancer Awareness. 2016 See http://www.moh.gov.sa/en/HealthAwareness/Campaigns/Breastcancer/Pages/stat.aspx (accessed 31 October 2018).

4. Martin TA, Ye L, Sanders AJ, Lane J, Jiang WG. 2013 Cancer invasion and metastasis: molecular and cellular perspective. In *Madame Curie Bioscience Database [Internet] 2000–2013*. Austin, TX: Landes Bioscience. Available from: https://www.ncbi.nlm.nih.gov/books/NBK164700/.

5. Schlessinger J. 2000 Cell signaling by receptor tyrosine kinases. *Cell* **103**, 211–225. (doi:10.1016/S0092-8674(00)00114-8)

6. Kwapisz D. 2017 Cyclin-dependent kinase 4/6 inhibitors in breast cancer: palbociclib, ribociclib, and abemaciclib. *Breast Cancer Res. Treat.* **166**, 41–54. (doi:10.1007/s10549-017-4385-3)

7. Bilgin B, Sendur MAN, Şener Dede D, Akıncı MB, Yalçın B. 2017 A current and comprehensive review of cyclin-dependent kinase inhibitors for the treatment of metastatic breast cancer. *Curr. Med. Res. Opin.* **33**, 1559–1569. (doi:10.1080/03007995.2017.1348344)

8. Kadi AA, Amer SM, Darwish HW, Attwa MW. 2017 LC-MS/MS reveals the formation of aldehydes and iminium reactive intermediates in foretinib metabolism: phase I metabolic profiling. *RSC Adv.* **7**, 36 279–36 287. (doi:10.1039/C7RA06341E)

9. Kadi AA, Attwa MW, Darwish HW. 2018 LC-ESI-MS/MS reveals the formation of reactive intermediates in brigatinib metabolism: elucidation of bioactivation pathways. *RSC Adv.* **8**, 1182–1190. (doi:10.1039/C7RA10533A)

10. Attwa MW, Kadi AA, Alrabiah H, Darwish HW. 2018 LC–MS/MS reveals the formation of iminium and quinone methide reactive intermediates in entrectinib metabolism: *in vivo* and *in vitro* metabolic investigation. *J. Pharm. Biomed. Anal.* **160**, 19–30. (doi:10.1016/j.jpba.2018.07.032)

11. Attwa MW, Kadi AA, Darwish HW, Alrabiah H. 2018 LC-MS/MS reveals the formation of reactive ortho-quinone and iminium intermediates in saracatinib metabolism: phase I metabolic profiling. *Clin. Chim. Acta* **482**, 84–94. (doi:10.1016/j.cca.2018.03.037)

12. Attwa MW, Kadi AA, Darwish HW, Amer SM, Al-shakliah NS. 2018 Identification and characterization of *in vivo*, *in vitro* and reactive metabolites of vandetanib using LC–ESI–MS/MS. *Chem. Cent. J.* **12**, 99. (doi:10.1186/s13065-018-0467-5)

13. Knowles SR, Uetrecht J, Shear NH. 2000 Idiosyncratic drug reactions: the reactive metabolite syndromes. *The Lancet* **356**, 1587–1591. (doi:10.1016/S0140-6736(00)03137-8)

14. Ju C, Uetrecht J. 2002 Mechanism of idiosyncratic drug reactions: reactive metabolites formation, protein binding and the regulation of the immune system. *Curr. Drug Metab.* **3**, 367–377. (doi:10.2174/1389200023337333)

15. Ma S, Zhu M. 2009 Recent advances in applications of liquid chromatography-tandem mass spectrometry to the analysis of reactive drug metabolites. *Chem. Biol. Interact.* **179**, 25–37. (doi:10.1016/j.cbi.2008.09.014)

16. Stepan AF, Walker DP, Bauman J, Price DA, Baillie TA, Kalgutkar AS, Aleo MD. 2011 Structural alert/reactive metabolite concept as applied in medicinal chemistry to mitigate the risk of idiosyncratic drug toxicity: a perspective based on the critical examination of trends in the top 200 drugs marketed in the United States. *Chem. Res. Toxicol.* **24**, 1345–1410. (doi:10.1021/tx200168d)

17. Kadi AA, Darwish HW, Attwa MW, Amer SM. 2016 Detection and characterization of ponatinib reactive metabolites by liquid chromatography tandem mass spectrometry and elucidation of bioactivation pathways. *RSC Adv.* **6**, 72 575–72 585. (doi:10.1039/C6RA09985H)

18. von Jagow R, Kampffmeyer H, Kiese M. 1965 The preparation of microsomes. *Naunyn Schmiedebergs Arch. Exp. Pathol. Pharmakol.* **251**, 73–87. (doi:10.1007/BF00245731)

19. Amer SM, Kadi AA, Darwish HW, Attwa MW. 2017 Identification and characterization of *in vitro* phase I and reactive metabolites of masitinib using a LC-MS/MS method: bioactivation pathway elucidation. *RSC Adv.* **7**, 4479–4491. (doi:10.1039/C6RA25767D)

20. Kadi AA, Darwish HW, Abuelizz HA, Alsubi TA, Attwa MW. 2018 Data from: Identification of reactive intermediates formation and bioactivation pathways in Abemaciclib metabolism by LC-MS/MS: *In vitro* metabolic investigation. Dryad Digital Repository. (doi:10.5061/dryad.71f1s18)